J. Chem. Sci. Vol. 129, No. 1, January 2017, pp. 81–93. © Indian Academy of Sciences.
DOI 10.1007/s12039-016-1203-0

REGULAR ARTICLE

Highly efficient catalytic reductive degradation of various organic dyes by Au/CeO_2-TiO_2 nano-hybrid

PRANJAL SAIKIA[a,*], ABU T MIAH[a] and PARTHA P DAS[b]
[a]Department of Applied Sciences (Chemical Science Division), GUIST, Gauhati University, Guwahati 781 014, Assam, India
[b]Department of Physics, NIT Karnataka, Surathkal, Mangalore 575 025, Karnataka, India
Email: psjorhat@gmail.com; pranjalsaikia@gauhati.ac.in

MS received 27 August 2016; revised 1 November 2016; accepted 1 November 2016

Abstract. Highly improved catalytic reductive degradation of different organic dyes, in the presence of excess $NaBH_4$ over Au/CeO_2-TiO_2 nano-hybrid as the catalyst is reported in this study. CeO_2-TiO_2 nanocomposite was prepared by a facile co-precipitation method using ultra-high dilute aqueous solutions. Small amount of Au (only 1 wt%) was loaded onto the nanocomposite material by deposition-precipitation with urea (DPU) method to fabricate the ternary Au/CeO_2-TiO_2 nano-hybrid. The catalysts were characterized by the representative techniques like XRD, BET surface area, ICP-AES, UV-Vis diffuse reflectance spectroscopy, TEM and XPS. The Au/CeO_2-TiO_2 nano-hybrid along with $NaBH_4$ exhibited remarkable catalytic activities towards all the probed dyes, namely Methylene Blue, Methyl Orange, Congo Red, Rhodamine B and Malachite Green, with a degradation efficiency of ~100% in a short reaction time. The degradation reaction followed pseudo-first-order kinetics with respect to the concentration of the dye. Different parameters that affect the rate of the reaction are discussed. A plausible mechanism for methylene blue degradation has also been proposed.

Keywords. Nanocomposite; gold nanoparticles; Au/CeO_2-TiO_2; organic dye; catalytic reduction; nano-hybrid.

1. Introduction

Synthetic organic dyes and pigments discharged from various industries are responsible for causing substantial environmental pollution as they cannot be degraded by conventional water treatment processes due to their complex aromatic structures, hydrophilic nature and high stability against light, temperature, water, chemicals, *etc*.[1,2] In this view, degradation of organic dye molecules in waste water has gained paramount attention.[1,3] Till date, several techniques such as physical methods (*e.g*., precipitation, adsorption, and reverse osmosis), chemical methods (*e.g*., oxidation using O_2, O_3, NaOCl, and H_2O_2 as oxidants and reduction using $Na_2S_2O_4$), and biological methods (aerobic and anaerobic treatments) have been developed and employed for the treatment of such dye-containing waste water.[4] However, due to pricey set up, relentless energy input, low efficiency of dye removal and discharge of massive amount of sludge and toxic intermediates to environment, these techniques lack practical utility.[1,5] Though photocatalytic oxidative degradation of organic dyes and pollutants is an effective way, these processes are also slow and inherently energy consuming. On the contrary, catalytic reduction is a relatively fast process.

Catalytic reductive degradation of organic dye molecules by metal nano particles (MNPs) in the presence of $NaBH_4$ occurs by an electron transfer process. MNPs could make the process kinetically feasible by lowering the activation energy.[6,7] In these processes, there may be a large redox potential difference between the electron donor (BH_4^- ion) and acceptor (dyes) species, which can hamper relaying of electrons.[6–8] Interestingly, MNPs are viable enough to reduce the potential difference because of their high Fermi potentials for which they can exhibit excellent dye degradation efficiency.[2,6–9] Therefore, design and synthesis of catalytic material possessing suitable redox potential between the electron donor and acceptor species to act as an efficient electron relay system is challenging and of utmost importance. Among the diverse MNPs, the noble metal NPs (e.g., Au, Ag, Pt, and Pd) have been able to gain tremendous importance in catalytic dye degradation because of their good electron relaying capability arising from their appropriate redox potentials.[6,8,10–13] Besides, these NPs are practically more effective in degrading most of the dyes in waste water than many of the conventionally used methods.

*For correspondence

However, nano-sized metal particles are intrinsically unstable and prone to agglomerate to minimize their surface area due to van der Waals forces and high surface energy, which leads to lowering of their catalytic activity.[2,14–16] In addition, they cannot be easily isolated from the reaction mixture by simple filtration or centrifugation technique which restricts their large scale applications due to high cost and limited resources. So, use of MNPs directly in waste water treatment faces prohibitive challenges. Various sorts of polymers, complexing agents and surfactants are frequently used to stabilize the metal NPs.[6,14,16–18] However, the prime disadvantage of using such stabilizing agents for devising MNPs is their lower catalytic activity.[14,16] In addition, the surfactant coated MNPs do not settle down under gravity and hence involve energy and time consuming processes such as centrifugation and filtration for their recovery. As a result, their separation becomes tedious and expensive, which is unfavorable for recycling of catalysts. In order to stabilize the MNPs, lately, they have been anchored onto various solid supports (such as polymer, carbon, metal oxides and so on) to form composite catalysts so that they are fixed in place which reduces the chances of rapid agglomeration and promote the ease of settling down permanently.[8,15,16]

Of the various solid oxide materials explored, CeO_2 based oxides have been specially recognized as one of the most effective supporting oxides for stabilizing Au NPs because of the strong metal support interaction (SMSI) effect between them.[19–22] As a result, these materials promote elevated dispersion and stabilization of the Au NPs delivering more Au atoms to the reactants, thereby enhancing catalytic activity.[21,22] Nowadays, hybrid nanomaterials are devised which combine the advantages of two or more components to afford desirable properties. Because of this, they are becoming one of the extensively studied materials in chemistry, environmental pollution treatment, biomedical applications and so on.[23–25] Therefore, in this work, we have paid attention to improve the catalytic activity and stability of Au NPs by combining various components. Accordingly, we have chosen CeO_2-TiO_2 nanocomposite as the supporting material for attaching Au NPs because of its representative features: (a) the particles of CeO_2-TiO_2 nanocomposite possess good structural and thermal stability and hence obstruct sintering tendency of their particles,[26–28] (b) the Ce^{3+}/Ce^{4+} redox couple of CeO_2, with its ability to fluctuate between CeO_2 and Ce_2O_3 favors its catalytic activity under oxidizing and reducing environments, respectively,[1,29,30] (c) the increased BET surface area upon incorporation of two different oxides assists diffusion of the reactant into the bulk of the catalyst and hence provides fast intra-particle molecular transfer,[27,30] and (d) incorporation of CeO_2 with TiO_2 increases the amount of surface chemisorbed oxygen species, which can easily capture electrons and yield surface oxygen radicals with excellent reduction capability.[26,27]

Based on the above cited features, several studies have been performed using CeO_2-TiO_2 nanocomposite as an efficient photocatalyst in the degradation of various organic dyes[26,30] or in heterogeneous catalysis as noble metal catalyst support.[29,31] In the previous study, we observed excellent catalytic activity of nanosized, Au-supported CeO_2-based composite in the conversion of 4-nitrophenol to 4-aminophenol.[32] Recently, Sudarsanam *et al*., studied the CO oxidation reaction catalyzed by Au/Ce-TiO_2.[33] Zhang *et al.*, performed visible light driven selective photoelectrocatalytic aerobic benzyl alcohol oxidation over Au-deposited CeO_2-TiO_2 nanotubes.[34] At this point, it is imperative to mention that the degradation of Methylene Blue (MB) *via* $NaBH_4$ with Au-supported ceria-based solid catalysts have not been reported. Especially, much less attention has been devoted on the catalytic degradation of any kind of dye pollutants utilizing Au/CeO_2-TiO_2 composite catalyst materials. Herein, we embedded Au NPs onto the binary CeO_2-TiO_2 with the intention to utilize the beneficial features of both CeO_2-TiO_2 and Au NPs as the latter can promote reduction of dye molecules by relaying electrons in presence of $NaBH_4$. We avoided the use of any sort of protective agents for embedding Au NPs onto the CeO_2-TiO_2 nanocomposite and adopted deposition-precipitation with urea method because urea is an environmentally friendly precipitant having the capability of producing smaller Au particles. Apart from MB, reduction of other four organic dye pollutants of different characteristics such as methyl orange (MO), congo red (CR), rhodamine B (RhB), and malachite green (MG) were tested for demonstrating the exceptional catalytic efficacy of the nano-hybrid. Kinetic studies were performed to obtain apparent rate constants of the different degradation reactions. Activity parameters (K, min^{-1} g^{-1}) for all the reactions were also calculated. As far as we are aware, this might be the first study wherein Au NP-decorated CeO_2-TiO_2 nanocomposite is being employed in the catalytic reductive degradation of different organic dyes using $NaBH_4$ as a reducing agent.

2. Experimental

2.1 *Materials*

All the chemicals used in this study were of analytical grade and we used them as received. $(NH_4)_2Ce(NO_3)_6$,

$HAuCl_4.3H_2O$, MB, MO, CR, RhB, and MG were acquired from Himedia (India). NH_3, NH_2CONH_2, $BaSO_4$ and $NaBH_4$ were obtained from Merck. $TiCl_4$ was purchased from Sigma-Aldrich.

2.2 *Methods*

2.2a *Synthesis of Au/CeO_2-TiO_2 nano-hybrid*: The synthesis details were reported previously.[19,20] In brief, first we prepared CeO_2-TiO_2 composite oxide by co-precipitation method using ultra-high dilute aqueous solutions of $(NH_4)_2Ce(NO_3)_6$ and $TiCl_4$ with their appropriate amounts (1:1 mole ratio based on their oxides). Dilute NH_3 solution was used as the precipitant (pH = 8.5) in this step. The CeO_2-TiO_2 composite oxide thus formed was further used as the supporting material for deposition of nano-sized Au (1 wt%) particles onto it by conventional deposition-precipitation with urea (DPU) technique. In this case, urea was used as the precipitating material maintaining the ratio of [urea]:[Au] at 100. The final catalyst Au/CeO_2-TiO_2 obtained by this technique was calcined at 400°C for 12 h under air atmosphere.

2.2b *Catalyst characterization*: The BET surface areas were determined by N_2 physisorption at liquid N_2 temperature on a Micromeritics Gemini 2360 instrument using a thermal conductivity detector (TCD). The powder X-ray diffraction (XRD) patterns were recorded on a Rigaku Multiflex instrument using nickel-filtered CuK_α (0.15418 nm) radiation source and a scintillation counter detector. The intensity data were collected over a 2θ range of 10–80°. UV–Vis diffuse reflectance spectra were recorded on a UV–Visible spectrophotometer, Model U-4100 spectrophotometer. The UV-Vis DR spectra were recorded for the solid samples with $BaSO_4$ as the reference material in the range of 200–800 nm. Transmission electron microscopic (TEM) investigations were made on a JEM-2100 (JEOL) instrument equipped with a slow scan CCD camera. XPS studies were carried out on a V-G Microtech unit ESCA 3000 Spectrometer with two anodes, AlK_α (1486.6 eV) and MgK_α (1256.6 eV). The recorded XPS spectra were charge corrected with respect to the C 1s peak at 284.6 eV. Inductively coupled plasma-atomic emission spectroscopy (ICP-AES) measurement was performed (Model: ARCOS M/s. Spectro, Germany) in order to estimate the actual Au content of the nano-hybrid.

2.2c *Evaluation of catalytic activity*: We employed the Au/CeO_2-TiO_2 nano-hybrid for investigating reductive degradation of five organic dyes (apart from MB, two anionic and two cationic dyes) by using $NaBH_4$ as the reducing agent. The reaction was performed at 30 ± 1°C in aqueous medium. The temperature was maintained by circulating cold water around the reaction vessel. The degradation process was monitored with the help of UV-Vis spectrophotometer by recording the decrease of respective absorbance maxima. In a specific reaction procedure, 30 mL of aqueous dye solution was mixed with 2 mL of 0.2 M $NaBH_4$. Then, certain amount of the nano-hybrid catalyst was added into the above solution and the whole mixture was left for continuous mild stirring. After definite intervals of time, an aliquot of the solution was transferred to a quartz cuvette and its UV-Vis absorbance spectrum was recorded. The extent of dye degradation was calculated using the relation:

$$\text{Degradation}\% = [(A_o - A_t)/A_o] \times 100\%$$

where, A_o is the initial absorbance of dye solution and A_t is the absorbance at different time intervals.

3. Results and Discussion

3.1 *Characterization of catalysts*

The X-ray diffraction patterns of the synthesized samples are presented in Figure 1. As can be seen, the 2θ positions of the diffraction peaks for the both samples clearly demonstrate the presence of pure CeO_2 crystal phase with cubic fluorite structure (ICDD No. 43-1002). The diffraction peaks seem to be quite broad, suggesting the presence of nano-crystalline CeO_2 particles. Besides, any diffraction peaks pertaining to TiO_2 phases were not detected. This result reveals that TiO_2 is present as the same phase with CeO_2. This again confirms the penetration of Ti atoms into the CeO_2 crystal lattice.[35]

Using the most intense CeO_2 (111) diffraction peak, the average particle size of CeO_2 nano-crystals was calculated with the help of Debye-Scherrer's equation (see Supplementary Information). The calculated values are 4.7 and 4.9 nm, respectively, for CeO_2-TiO_2 and Au/CeO_2-TiO_2 samples. In the XRD pattern of the Au/CeO_2-TiO_2 sample (Figure 1b) two small peaks could be observed at 2θ = 38.5° and 44.6°, respectively,

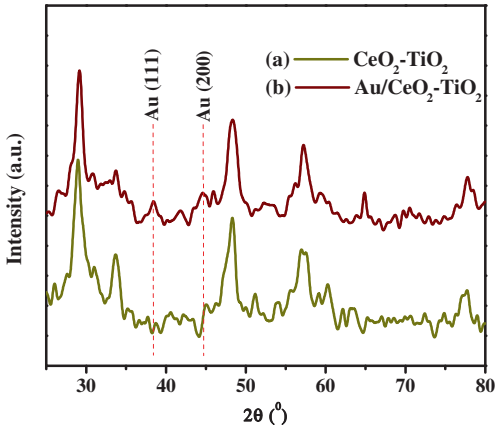

Figure 1. XRD patterns of (a) CeO_2-TiO_2, and (b) Au/CeO_2-TiO_2 nano-hybrid.

for (111) and (200) planes of face centered Au, signifying that the Au particles were finely dispersed on the CeO_2-TiO_2 nanocomposite surface (JCPDS: 04-0784).[36] Crystallite size of the Au NPs could not be calculated by using the Scherrer's formula because of low intensity of the Au diffraction peaks and hence TEM measurements were performed for the same. Interestingly, the positions of the diffraction peaks for the Au embedded sample, Au/CeO_2-TiO_2, were unaltered with respect to those for the standard data of CeO_2. However, intensity of the diffraction peaks were reduced a little, which is probably due to the low Au loading or high dispersion of Au species on the CeO_2-TiO_2 composite oxide surface. The actual Au content in the Au/CeO_2-TiO_2 sample was found to be 0.923 (in terms of wt% as determined by ICP–AES). Furthermore, specific surface areas of 80 and 75.15 m^2/g were obtained for the CeO_2-TiO_2 and Au/CeO_2-TiO_2 samples, respectively. The fall in the surface area after gold deposition was attributed to penetration of Au NPs into the pores of the support, thereby narrowing its pore diameter and blocking some of the micropores.[19,20]

The synthesized samples were analyzed by TEM in order to know their structural morphology. Figure 2 shows the TEM-HRTEM images of the samples. As can be seen in Figure 2a, the interplanar spacing of 0.30 nm corresponds to the (111) plane of cubic fluorite CeO_2 particles, which possess an average crystallite size of 5 nm with hemispherical shape. The measured crystallite sizes are satisfactorily in line with those obtained from XRD measurements. Figures 2b and c display the TEM images of Au/CeO_2-TiO_2 nano-hybrid. It is imperative to mention here that the detection of Au particles is hardly discernible from TEM images of CeO_2-based nano Au catalysts due to the poor contrast between CeO_2 and Au particles.[33,37] In this case, a closer inspection could make the Au particles noticeable as nearly spherical shaped dark contrasted zones (Figure 2c). Apart from this, the HRTEM image could make the Au particles more clearly distinct because the lattice spacing of 0.19 nm for (200) plane of Au particles differ from that of CeO_2 (Inset of Figure 2c). The Au particles possess good dispersion onto the surface of CeO_2-TiO_2 with almost regular size of ~4 nm

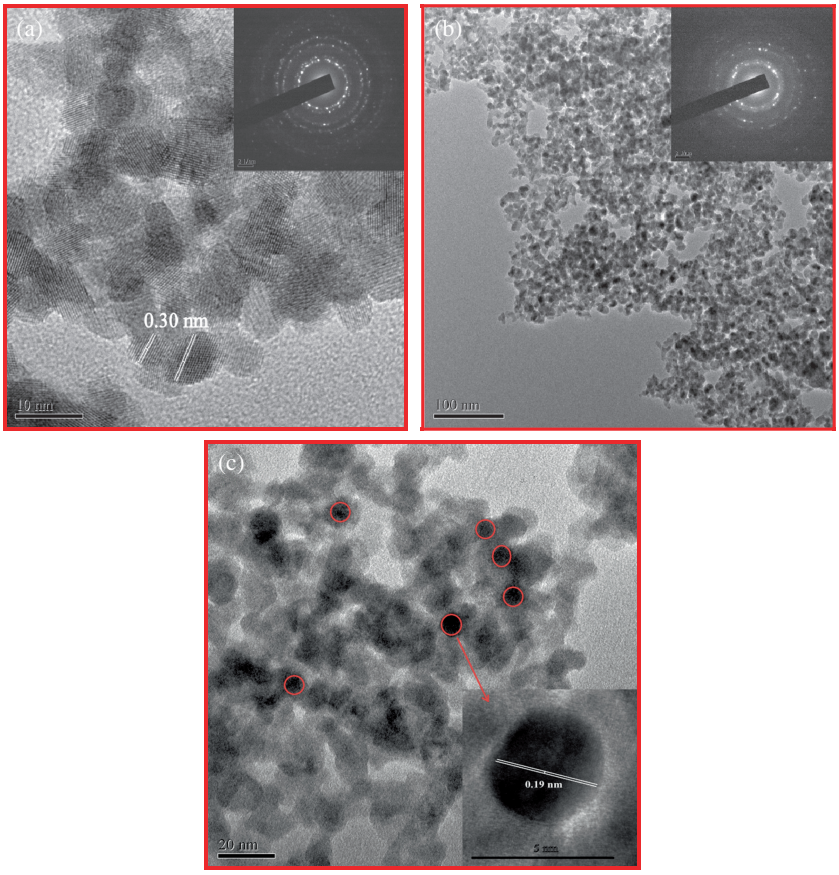

Figure 2. HRTEM image of CeO_2-TiO_2 nanocomposite (a), and TEM images of Au/CeO_2-TiO_2 nano-hybrid (b) and (c). SAED patterns of CeO_2-TiO_2, and Au/CeO_2-TiO_2 nano-hybrid are, respectively, shown as inset in Figure (a) and (b). Inset shown on the right hand bottom corner of (c) indicates HRTEM image of single Au NP.

(Figures 2b and c). Eventually, the selected area electron diffraction (SAED) patterns, shown as inset of Figures 2a and b, demonstrate the nano-crystalline nature of the prepared materials. Further observation is preservation of crystallinity of the CeO_2-TiO_2 nanocomposite after Au deposition which is in line with the XRD result.

The light absorption behavior of the samples was investigated by UV-Vis DRS analysis. The diffuse reflectance spectra are presented in Figure 3. The DR pattern (Figures 3a and b) exhibits three common absorption peaks centered at around 230, 290, and 335 nm for both samples. The first two bands can be assigned to $O^{2-} \rightarrow Ce^{3+}$ and $O^{2-} \rightarrow Ce^{4+}$ charge transfer transitions, respectively, while the latter one is due to inter-band transition.[20,38] These results demonstrate the co-existence of Ce^{3+} and Ce^{4+} ions in the synthesized samples, which is in line with our recently reported results.[19,20] Interestingly, the Au/CeO_2-TiO_2 sample exhibits an additional broad absorption peak in the visible region, that is, at ~535 nm (Figure 3b). This characteristic absorption peak is attributed to surface plasmon resonance (SPR) band of single metallic Au NPs.[39] This further substantiates that the Au NPs had been deposited successfully onto the CeO_2-TiO_2 nanocomposite surface. It is reported that positively charged $Au^{\delta+}$ species shows an absorption band at 275 nm for Au_n clusters ($1 < n < 10$).[40] Interestingly, we did not get any absorption band relating to cationic Au species in the DR spectrum of Au/CeO_2-TiO_2 nano-hybrid. To authenticate the DRS assumptions, XPS analysis of the samples was performed.

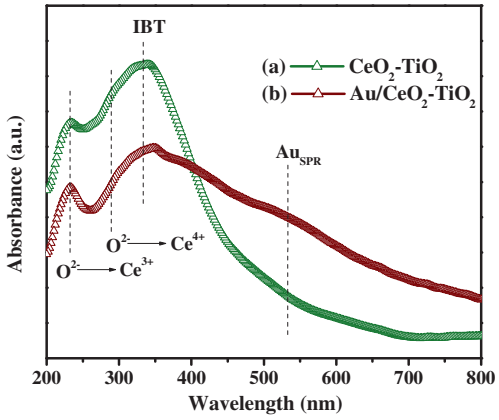

Figure 3. Diffuse reflectance UV-Vis spectrum of (a) CeO_2-TiO_2, and (b) Au/CeO_2-TiO_2 nano-hybrid.

Figure 4a depicts XPS survey scan spectrum of Au/CeO_2-TiO_2 nano-hybrid viewing that the material is mainly composed of Au, Ce, Ti, O, as well as C, and no other impurity element was detected in appreciable amount. High resolution X-ray photoelectron spectra of the detected elements were also recorded to get a clear insight into their valence states. As shown in Figure 4b, the binding energy (BE) peaks at 83.55 and 87.31 eV correspond to Au $4f_{7/2}$ and Au $4f_{5/2}$ states, respectively, suggesting the presence of zero valent (metallic) Au^o species on the surface of the CeO_2-TiO_2 nanocomposite. However, as per previous reports, BE values for Au^o species were observed at 84.0 and 87.7 eV, respectively, for the Au $4f_{7/2}$ and Au $4f_{5/2}$ states.[34,41] The lower BE values we obtained for the Au nano-hybrid may be due to high electron concentration around the Au particles attributable to transfer of electrons from oxygen vacancies of the CeO_2-TiO_2 to Au species.[34] Interestingly, BE peaks relating to cationic Au species such as Au^{3+} or Au^+ were not identified in the Au 4f photoelectron spectrum. Ce 3d spectrum (Figure S1a in Supplementary Information) showed multiple BE peaks. The set of peaks at ~883.37, 889.53, 898.94, 901.65, 907.80, and 917.04 eV, demonstrates the existence of Ce^{4+}, while the peaks at ~884.91 and 903.56 eV, confirm the presence of Ce^{3+}. The BE peaks at 458.12 and 463.85 eV, observed in Ti 2p photoelectron spectrum (Figure S1b) indicate the presence of Ti^{4+}.[42] The O 1s spectrum showed a broad peak at 530.00 eV, as presented in Figure S1c. This BE peak is attributed to lattice oxygen incorporating to CeO_2-TiO_2 nanocomposite.[38]

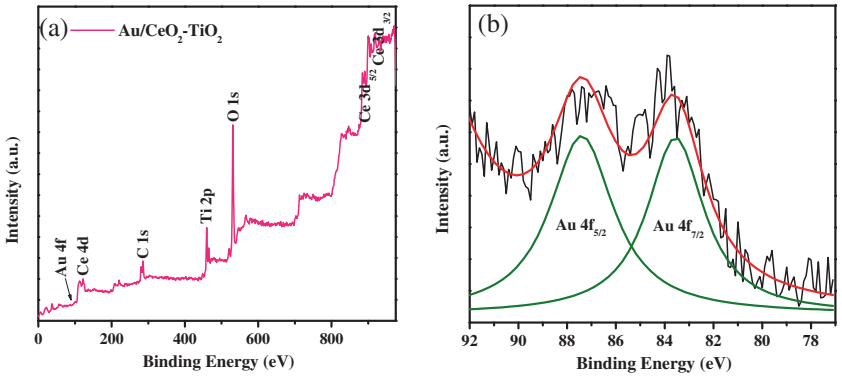

Figure 4. XPS survey spectrum of Au/CeO_2-TiO_2 nano-hybrid (a), and high resolution XP spectrum of Au 4f (b).

3.2 *Catalytic Reduction of Methylene Blue*

MB dye was selected as a model pollutant to investigate the catalytic performance of the Au/CeO_2-TiO_2 hybrid nano-catalyst with $NaBH_4$ as the reducing agent under ambient conditions. $NaBH_4$ was used as the reducing agent because of high electron injection capability of the BH_4^- ions.[43] It was seen that addition of Au/CeO_2-TiO_2 nano-hybrid and $NaBH_4$ rapidly diminished the blue color of MB solution to a colorless one, indicating its reduction to leucomethylene blue (LMB).[44] The MB absorption peak intensity at 664 nm decreased with the passage of time. The time-dependent UV-Vis spectra showing the reduction pattern of MB by $NaBH_4$ over the nano-hybrid is presented in Figure 5a. As can be seen from the figure, the absorption intensity became zero after 10.5 min, demonstrating the completion of the reaction. Figure 5b displays the decolorization of

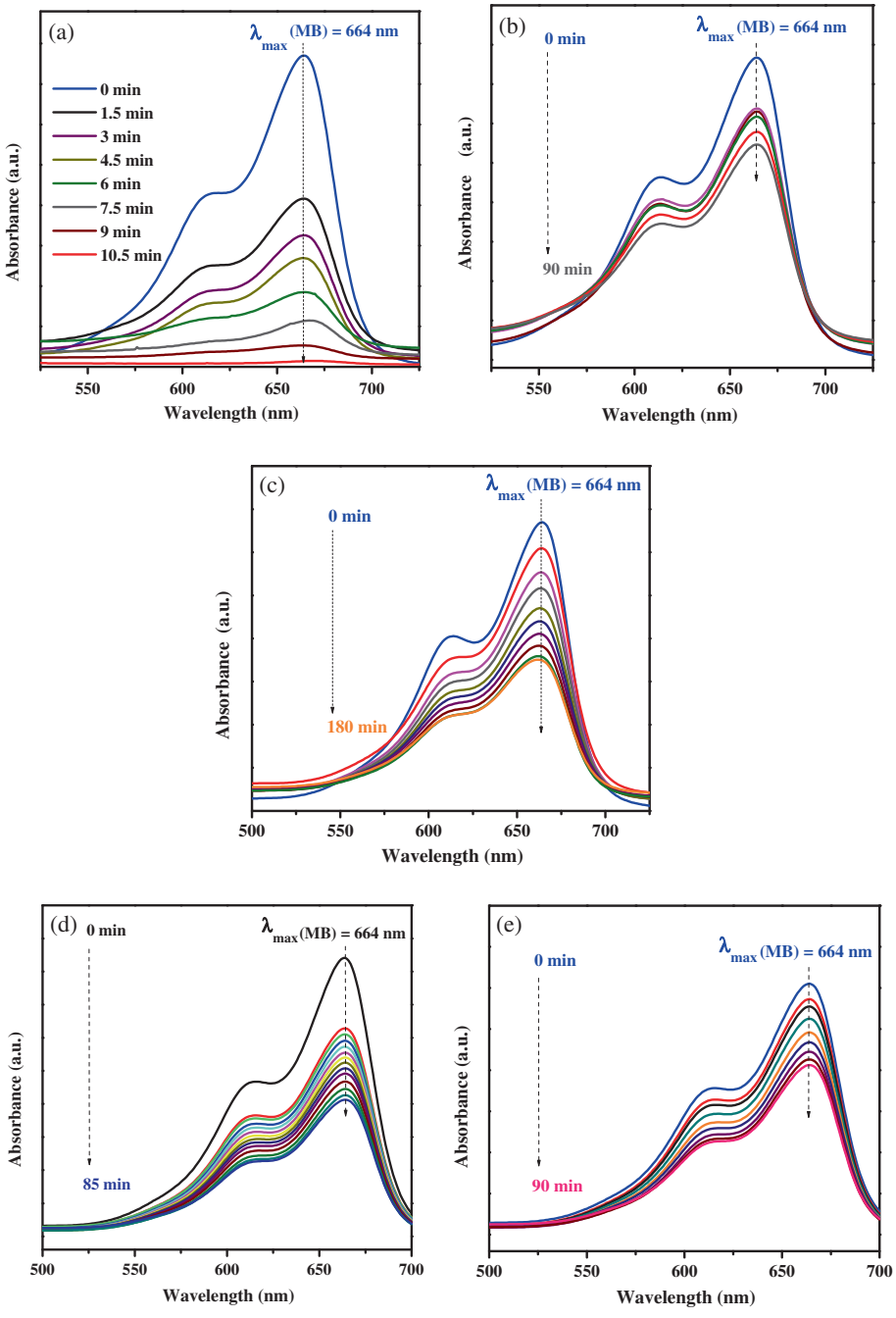

Figure 5. UV-Vis absorption spectra of aqueous MB (30 mL, 48.14×10^{-6} M) with, (a) 2 mL of 0.2 M $NaBH_4$ and 0.433 g/L of Au/CeO_2-TiO_2 nano-hybrid, (b) 2 mL of 0.2 M $NaBH_4$, (c) 0.433 g/L of Au/CeO_2-TiO_2 nano-hybrid, (d) 2 mL of 0.2 M $NaBH_4$ and 0.433 g/L of CeO_2-TiO_2 nanocomposite, and (e) 0.433 g/L of CeO_2-TiO_2 nanocomposite.

the dye only in the presence of $NaBH_4$. It was seen that $NaBH_4$ alone could not degrade the dye even after 90 min. Similarly, in the absence of $NaBH_4$, the nano-hybrid itself showed rather slower degradation efficiency (Figure 5c). This suggests that neither $NaBH_4$ nor the nano-hybrid alone is viable to catalyze the swift degradation of MB and the reaction could only be finished quickly when both the nano-hybrid and $NaBH_4$ were used together. Hence, it could be concluded that the nano-hybrid efficiently catalyzed the reduction of MB by relaying of electrons from BH_4^- species to MB *via* the Au NPs.[2,8,10,15,18,24,45] This assumption was further corroborated by conducting control experiments over bare CeO_2-TiO_2 nanocomposite with and without $NaBH_4$, which revealed insignificant catalytic activity (Figures 5d and 5e). However, other CeO_2-based Au catalysts such as Au/CeO_2 and Au/CeO_2-ZrO_2 showed comparatively poor MB reduction efficiencies under the same reaction conditions (Figures S2a and 2b, respectively, in Supplementary Information). Therefore, Au/CeO_2-TiO_2 was chosen as the working catalyst for carrying out the reduction of dyes other than MB in the present study.

The reduction of MB by Au/CeO_2-TiO_2 catalyst in the presence of $NaBH_4$ could be explained by Langmuir-Hinshelwood model, according to which, the initially adsorbed BH_4^- ions donate electrons to the Au NPs. As a result, a negatively charged layer is developed around the Au NPs.[16] Subsequently, the Au NPs transfer these electrons to MB molecules for setting off the reduction reaction at the surface of Au NPs.[46] Recently, Azad *et al.*, showed that in aqueous environment, the BH_4^- ions create a negatively charged layer around the Au NPs which facilitates the cationic dye MB to be adsorbed on the surface of Au NPs through electrostatic interaction.[18] Soon after that, Khan *et al.* also claimed the similar tendency of Au NPs in the presence of BH_4^- ions.[8] On these bases, we anticipated an analogous reaction between Au NPs and BH_4^- ions, developing a layer of negative charge around the Au/CeO_2-TiO_2 nano-hybrid as shown in equation (1).

$$BH_4^- + Au/CeO_2\text{-}TiO_2 + 3H_2O \rightarrow BO_3^{3-} + (Au/CeO_2\text{-}TiO_2)^{8-} + 10H^+ \quad (1)$$

This negative layer thus formed enables the Au particles to attract the MB dye strongly towards it and thus transfer of electrons to the dye molecules becomes very swift. In this reaction, $NaBH_4$ acts as a hydrogen supplier too. The hydrogen species generated from BH_4^- ions attack the MB molecules after electron transfer to Au NPs. This reaction leads to the reduced form of MB which is generally colorless.[2,6]

As per earlier literature reports, catalytic activity of noble metal nanoparticles (NMNPs) is incredibly improved when they are small sized and highly dispersed. This is because, the highly dispersed smaller NMNPs enable easy access of the target molecules to reach surface of NMNPs that serve as an electron relay in the reaction system.[45–48] However, this trend is not fully applicable in the case of Au NPs acting as electron relaying system. It is reported that Au NPs, when too large or small, cannot effectively relay electrons from BH_4^- ions to an electrophile and the particles ranging from 2–5 nm were thought to be appropriate for the same.[8,43] In our case, the TEM images showed good dispersion of small sized Au NPs (~4 nm in average) over CeO_2-TiO_2 nanocomposite surface that may be the reason for high catalytic activity of the nano-hybrid. The smaller Au NPs could have a high surface-to-volume ratio and thus rendered more Au atoms on the nanocomposite surface, which served as the active catalytic sites for MB reduction.[48] As MNP catalyzed reduction of dyes proceeds through an electron transfer process, the rate of such a reaction greatly depends on the swiftness of the process. The standard redox potential of Ce^{4+}/Ce^{3+} couple is 1.44 V, while that of Ti^{4+}/Ti^{3+} is 1.38 V. Hence, the transfer of electrons from Ti^{3+} to Ce^{4+} is thermodynamically favored. In presence BH_4^- ions, Ce^{4+} can undergo redox cycling to generate Ti^{3+}. This thermodynamically favored competitive redox reaction between CeO_2 and TiO_2 (*i.e.*, $Ce^{4+} + Ti^{3+} \leftrightarrow Ce^{3+} + Ti^{4+}$) in BH_4^- systems speeds up the electron transfer between the adsorbed molecules on the metallic Au surface resulting in an enhanced degradation of MB by the Au nano-hybrid.[24,32] Meanwhile, the local electron density built up around the Au NPs owing to electron transfer from oxygen vacancies of CeO_2-TiO_2 nanocomposite to Au facilitates the uptake of electrons by MB molecules from the nano-hybrid catalyst (evidenced from XPS).[32,34] Generally, nano-sized Au particles grown onto the different oxides possess either zero or positive (+1/ + 3) valence state. The cationic Au particles are electron scavengers and hence it is rational to expect that the electrons furnished by BH_4^- ions have the tendency to be retained with the Au particles rather than relaying them to the dye molecules for bringing about reduction. Therefore, lower catalytic activity might be experienced with cationic Au species in such kind of reduction reactions. In contrast, metallic Au (Au^o) particles have quite high ability to relay electrons to the dye molecules. Herein, the nano-hybrid contains Au^o particles which assists in the relaying of electrons and thereby efficiently catalyzing the reduction of MB. A schematic diagram for MB degradation

mechanism has been proposed on these bases as depicted in Figure S3 (Supplementary Information).

3.3 *Effect of operational parameters*

3.3a *Effect of catalyst loading*: In order to investigate the effect of catalyst loading on degradation of MB, we carried out four reactions by varying the amount of Au/CeO_2-TiO_2 nanohybrid from 0.183 to 0.433 g/L and keeping other two reaction parameters constant. The degradation profiles of aqueous MB (48.14×10^{-6} M) solution over the different nano-hybrid amounts along with $NaBH_4$ (0.2 M, 2 mL) solution is shown in Figure S4a–d (Supplementary Information). It was seen that the degradation efficiency increases as the nano-hybrid loading increases from 0.183 to 0.433 g/L. This is attributed to the higher availability of surface active sites for the adsorption of BH_4^- ions and the dye molecules with the increase in nano-hybrid loading[48,49] Therefore, the catalyst loading of 0.433 g/L was taken for investigating the other reaction parameters. As the concentration of $NaBH_4$ was in large excess compared to that of MB, hence the degradation process followed a pseudo-first-order kinetics. This can be expressed by the equation: $\ln(A_t/A_o) = k_{app}$ t. Thus, the plot of $\ln(A_t/A_o)$ vs. time for degradation of MB over different amounts of Au/CeO_2-TiO_2 nano-hybrid is a straight line as shown in Figure 6.

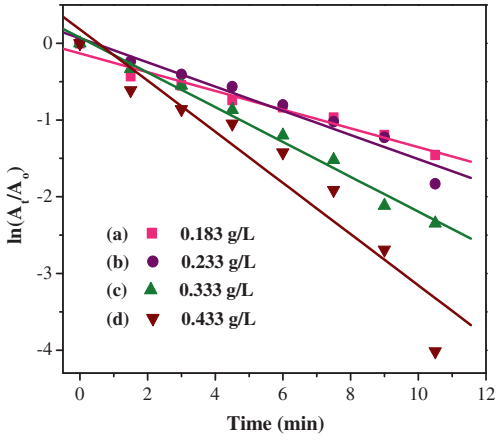

Figure 6. $\ln(A_t/A_o)$ vs. time plot of pseudo-first-order reaction kinetics for the degradation of MB with different catalyst loading: (a) 0.183 g/L, (b) 0.233 g/L, (c) 0.333 g/L, and (d) 0.433 g/L, with 2 mL of 0.2 M $NaBH_4$.

The apparent rate constants (k_{app}) were calculated from the slope of the linear plots. The overall results obtained for different nano-hybrid amounts are summarized in Table 1, which showed increase in the rate constants (k_{app}) and activity parameter (K $min^{-1}g^{-1}$) with catalyst loading.

3.3b *Effect of initial MB concentration*: In this study, four aqueous MB solutions of different concentrations ranging from 48.14×10^{-6} to 74.89×10^{-6} M were used with fixed concentration of the Au/CeO_2-TiO_2 nano-hybrid (0.433 g/L) and $NaBH_4$ (0.2 M, 2 mL). The corresponding UV-Vis absorption spectra for the degradation of MB with the stipulated concentrations are presented in Figure S5a–d (Supplementary Information). As can be seen, the time required for complete degradation increased with increasing concentration of MB. That is, the rate of the degradation decreased with increasing concentration of MB, which supports first-order-kinetics of the degradation process. This decrease in rate is due to the slowing down of the electron transfer process on the nano-hybrid surface

Table 1. Summary of different reaction parameters such as initial MB concentration, catalyst loading, and $NaBH_4$ concentration on the degradation of MB and, the obtained apparent rate constant (k_{app}) and activity parameter (K).

MB conc. (10^{-6} M)/30 mL	Catalyst loading (g/L)	$NaBH_4$ conc. (M)	Au conc. (10^{-6} M)	App. rate const. (k_{app}, 10^{-3} min^{-1})	Activity parameter (K, min^{-1} g^{-1})	Correlation co-efficient (R^2)[a]
48.14	0.183	0.2 × 2 mL	6.77	122.2	22.22	0.98
48.14	0.233	,,	11.81	157.7	22.52	0.97
48.14	0.333	,,	16.92	226.9	22.7	0.99
48.14	0.433	,,	22	333.6	25.66	0.95
58.84	0.433	,,	,,	295.6	22.73	0.98
66.86	0.433	,,	,,	194.7	14.98	0.99
74.89	0.433	,,	,,	171.4	13.19	0.99
48.14	0.433	0.125 × 2 mL	,,	168.3	12.94	0.98
48.14	0.433	0.150 × 2 mL	,,	192.8	14.83	0.98
48.14	0.433	0.175 × 2 mL	,,	252.3	19.41	0.98
48.14	nil	0.2 × 2 mL	nil	3.71	–	0.98
48.14	0.433	nil	,,	3.69	0.2838	0.99

[a]Correlation coefficients of the pseudo-first-order kinetic plots for MB degradation.

between $NaBH_4$ and MB dye. The pseudo-first-order kinetic plots for various MB concentrations are presented in Figure 7, and the apparent rate constant (k_{app}) as well as activity parameter (K $min^{-1}g^{-1}$) values are listed in Table 1.

3.3c *Effect of $NaBH_4$ concentration*: The amount of $NaBH_4$ influences the reduction of dye substances and in this view, the concentration of $NaBH_4$ was varied in order to determine the precise concentration for optimum degradation of MB dye. The related UV-Vis absorption spectra are presented in Figure S6a–d (Supplementary Information). In this case, the nano-hybrid dosage and MB concentration were fixed at 0.433 g/L and 4814 $\times$ 10^{-6} M, respectively, and the $NaBH_4$ concentration was varied from 0.125 to 0.2 M. It was found that the extent of degradation increases upon increasing $NaBH_4$ concentration. A complete degradation was observed in the presence of 0.2 M $NaBH_4$ at the prescribed reaction time. Therefore, 0.2 M was chosen as the critical $NaBH_4$ concentration. This observation suggests that an appropriate concentration of BH_4^- ions is imperative for achieving the best degradation efficiency of the Au/CeO_2-TiO_2 nano-hybrid. In fact, higher concentration of the $NaBH_4$ augmented local electron density on the surface of Au NPs that could lead to an increasing reaction rate.[50] The plot of $\ln(A_t/A_o)$ vs. time for MB degradation with a range of $NaBH_4$ concentrations are presented in Figure S6e (Supplementary Information), and the apparent rate constant (k_{app}) as well as activity parameter (K $min^{-1}g^{-1}$) values are summarized in Table 1. The $\ln(A_t/A_o)$ vs. time plot for MB degradation only with $NaBH_4$ or the nano-hybrid is also shown in Figure S7a and 7b (Supplementary Information). The rate constants were 0.00371 and 0.00369 min^{-1} only with $NaBH_4$ or the nano-hybrid, respectively. Thus, the rate of MB degradation enhances by more than ninety times when both the components are used together. Based on the above discussion, it could be concluded that all the three parameters are individually very important for obtaining a fast reduction of MB over the Au/CeO_2-TiO_2 nano-hybrid.

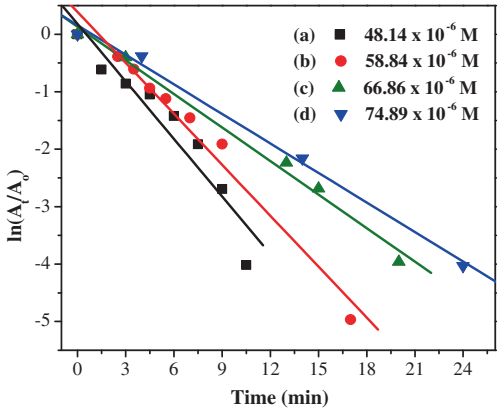

Figure 7. $\ln(A_t/A_o)$ vs. time plot of pseudo-first-order reaction kinetics for degradation of MB for different concentration: (a) 48.14 $\times$ 10^{-6} M, (b) 58.84 $\times$ 10^{-6} M, (c) 66.86 $\times$ 10^{-6} M, and (d) 74.89 $\times$ 10^{-6} M, 2 mL of 0.2 M $NaBH_4$ and 0.433 g/L of Au/CeO_2-TiO_2 nano-hybrid.

Some recent results dealing with the supported and/or unsupported MNP catalyzed reduction of MB in presence of $NaBH_4$ have been summarized in Table S1[2,8,46,51–58] (Supplementary Information) for giving an insightful comparison to our work in order to show the superior catalytic efficiency and advantages of the Au/CeO_2-TiO_2 catalyst. It is obvious from the table that our catalytic system is advanced in comparison to most of the previously reported results in view of some striking parameters, such as low percentage of Au loading, simple reaction conditions for preparation of catalysts, use of benign precipitant urea, low catalyst loading, avoidance of surfactant and/or polymer molecules, *etc*. Above all, the high activity which is the most enviable aspect of any catalyst was met with Au/CeO_2-TiO_2 making it an appropriate choice for MB degradation.

3.4 *Catalytic reduction of other dyes*

Apart from MB, we investigated the reductive degradation of other four organic water contaminants having different chemical structures, two anionic (MO and CR) and two cationic (RhB and MG) dyes, in order to demonstrate the extended reduction capability of our synthesized Au/CeO_2-TiO_2 nano-hybrid. The degradation reactions were monitored spectrophotometrically by following the decrease of absorbance of the dyes at their highest wavelength, λ_{max} [λ_{max}(MO) = 464 nm, λ_{max}(CR) = 498 nm, λ_{max} (RhB) = 553 nm, λ_{max} (MG) = 616 nm] with respect to time. The specific reaction conditions adopted here for performing the reductions are outlined in Table 2. Each of the reactions was separately performed only by adding $NaBH_4$ into the dye solutions. It was seen that $NaBH_4$ alone could not finish the reduction up to a long period of time (Figure S8a–d, Supplementary Information). However, all the reduction reactions were completed within few minutes when the nano-hybrid along with $NaBH_4$ was added to the dye solutions. This ensures that the catalyst is providing a surface for the adsorption of both dye molecules and BH_4^- ions, which boosts the rate of reduction by increasing relaying of electrons from BH_4^- ions to the dyes *via* the Au NPs. Thus, the nano-hybrid acts as an effective catalyst towards the reduction of all these dyes. The corresponding time-dependent

Table 2. Summary of reaction time (min), apparent rate constant (k_{app}), and activity parameter (K) for Au/CeO_2-TiO_2 nano-hybrid catalyzed reduction of MO, CR, RhB, and MG dye in the presence of $NaBH_4$.

Dye conc. (M)/30 mL	Catalyst loading (g/L)	Amount of $NaBH_4$	Reaction time (min)	App. rate const. (k_{app}, 10^{-3} min^{-1})	Activity parameter (K, min^{-1} g^{-1})	Correlation co-efficient (R^2)
MO (61.10×10^{-6})	0.566	0.2 M × 2 mL	7.5	433.7	25.51	0.99
MO (61.10×10^{-6})	nil	„	90	1.2	–	0.99
CR (28.71×10^{-6})	0.633	„	10	361.5	19.03	0.92
CR (28.71×10^{-6})	nil	„	90	1.95	–	0.99
RhB (10.44×10^{-6})	0.633	„	10	223.9	11.79	0.98
RhB (10.44×10^{-6})	nil	„	60	8.9	–	0.99
MG (54.81×10^{-6})	0.6333	0.01 M × 0.3 mL	14	233.2	12.27	0.93
MG (54.81×10^{-6})	nil	„	90	3.39	–	0.99

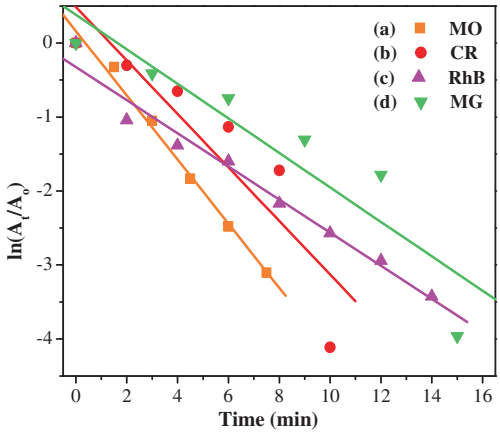

Figure 8. Pseudo-first-order kinetic plot of $\ln(A_t/A_o)$ vs. time for the reduction of (a) MO, (b) CR, (c) RhB, and (d) MG, catalyzed by Au/CeO_2-TiO_2 nano-hybrid in the presence of $NaBH_4$.

UV-Vis absorption spectra showing the reduction profiles of the dyes are presented in Figure S9a–d (Supplementary Information). It was seen that, within 7.5–15 min, complete reduction took place, depending on the type of dye molecules. The reduction process followed pseudo-first-order kinetic pathway as in the case of MB reduction (section 3.2). The apparent rate constants (k_{app}) for the reductions were calculated from the slope of the linear plots of $\ln(A_t/A_o)$ vs. time (Figure 8) and the values are presented in Table 2.

Among the different dyes, reduction of MO was the fastest, probably due to its better adsorption onto the nano-hybrid surface compared to other dyes. The appropriate reasons for the different reduction rates observed for the different dyes is still not clear and hence, further study is needed to explore such catalytic dye reduction phenomena. However, the difference in the reaction rate may be due to different chemical structures, charge, hydrophobicity, presence of donor atom, reduction potential, *etc*., which vary the activation energy for catalytic reduction reaction.[8,18,59] Interestingly, reduction efficiency of the nano-hybrid towards all the five dyes was found comparable to or even better than earlier work.[51,52,60,61] Such high activity of the material projects it as one of the viable platforms for not only reduction of dye substances but also for other promising applications.[17,23–25,39,62]

3.5 *Stability and reusability of the Au/CeO_2-TiO_2 nano-hybrid*

The stability and reusability of Au/CeO_2-TiO_2 nano-hybrid was investigated for MB reduction up to five cycles. After every cycle, the nano-hybrid was recovered from the reaction mixture by centrifugation and washed thrice with ethanol and water. The as-obtained sample was thereafter dried and reused for the next cycle of catalysis. It was seen that degradation (%) of MB by the regenerated nano-hybrid was nearly equal to that of the fresh catalyst even after its repetitive use (Figure S10a, Supplementary Information). The slight reduction in the degradation (%) might be due to the loss of catalyst during separation as the number of reactive surface sites for adsorption of MB and BH_4^- decreases with decreasing nano-hybrid amount. The nano-hybrid recovered after 5th cycle was analyzed by XRD and TEM technique to observe if there is any structural change occurred after the catalytic reaction. The XRD pattern of the reused catalyst was similar to that of the fresh catalyst (Figure S10b). TEM analysis revealed the formation of relatively larger particles giving the impression of agglomeration of smaller particles after repeated use (Figure S10c). However, ICP-AES analysis of the recycled nano-hybrid did not reveal any significant loss of Au. The overall observations validate that the anchored Au NPs are well-attached to the CeO_2-TiO_2 surface. Therefore, Au/CeO_2-TiO_2 nano-hybrid is an excellent catalyst with good reusability as well

as stability for the reduction of organic dyes, which imparts the prospect for its practical applications.

4. Conclusions

In summary, we could devise a highly efficient ternary nano-hybrid catalyst, Au/CeO_2-TiO_2, by utilizing facile and economic synthesis protocol which showed excellent dye reduction ability in the presence of $NaBH_4$ *via* an electron relaying process. The reduction followed pseudo-first-order kinetics and the rate of the reaction greatly depends on concentration of the dye, $NaBH_4$ and that of the nano-hybrid. The CeO_2-TiO_2 composite oxide used in this study worked as the stabilizing platform for the nano-sized Au particles. In addition, the thermodynamically favored redox reaction between the cationic Ce and Ti species accelerated the rate of reduction by speeding up electron relaying process. The metallic character of the Au particles residing onto CeO_2-TiO_2 composite assisted in the relaying of electrons and efficiently reduced the dyes. The excellent catalytic activity, stability and good reusability suggest that the Au/CeO_2-TiO_2 nano-hybrid could be used as potential candidate for the treatment of industrially discharged waste water. However, it is noted that mere color change may sometimes be deceptive to judge the effectiveness of dye removal. Therefore, systematic studies are necessary to draw any reasonable consensus.

Supplementary Information (SI)

Additional information such as XP spectrum of Ce 3d, Ti 2p, and O1s (Figure S1), mechanism of MB reduction (Figure S2), catalyst loading effect (Figure S3), MB concentration effect (Figure S4), $NaBH_4$ concentration effect and analogous $\ln(A_t/A_o)$ vs. time plot (Figure S5), $\ln(A_t/A_o)$ vs. time plot for MB reduction with only $NaBH_4$ and only Au/CeO_2-TiO_2 (Figure S6), reduction of MO, CR, RhB, and MG with only $NaBH_4$ (Figure S7) and with Au/CeO_2-TiO_2 and $NaBH_4$ (Figure S8), reusability, XRD, and TEM of Au/CeO_2-TiO_2 (Figure S9) and comparison of MNP catalyzed reduction of MB with the present work (Table S1) are provided in the supplementary information which is available at www.ias.ac.in/chemsci.

Acknowledgements

The authors are highly grateful to Department of Science and Technology, Govt. of India for research grant (SR/FT/CS-69/2011). Thanks are also due to NEHU (Shillong, Meghalaya, India), USIC-Gauhati University (Assam, India), and NCL Pune (Maharashtra, India) for giving us the opportunity to perform TEM, XRD, and XPS analyses, respectively. Help from Dr. L. Borah and Dr. K. K. Senapati is gratefully acknowledged.

References

1. Li H, Wang G, Zhang F, Cai Y, Wang Y and Djerdj I 2012 Surfactant-assisted synthesis of CeO_2 nanoparticles and their application in wastewater treatment *RSC Adv.* **2** 12413
2. Ghosh B K, Hazra S, Naik B and Ghosh N N 2015 Preparation of Cu nanoparticle loaded SBA-15 and their excellent catalytic activity in reduction of variety of dyes *Powder Technol.* **269** 371
3. El-Sharkawy E A, Soliman A Y and Al-Amer K M 2007 Comparative study for the removal of methylene blue via adsorption and photocatalytic degradation *J. Colloid Interface Sci.* **310** 498
4. Singh K and Arora S 2011 Removal of synthetic textile dyes from wastewaters: A critical review on present treatment technologies *Crit. Rev. Env. Sci. Technol.* **41** 807
5. Amaral P F F, Fernandes D L A, Tavares A P M, Xavier A B M R, Cammarota M C, Coutinho J A P and Coelho M A Z 2004 Decolorization of dyes from textile wastewater by trametes versicolor *Environ. Technol.* **25** 1313
6. Gupta N, Singh H P and Sharma R K 2011 Metal nanoparticles with high catalytic activity in degradation of methyl orange: An electron relay effect *J. Mol. Catal. A- Chem.* **335** 248
7. Mallick K, Witcomb M J and Scurrell M S 2005 Redox catalytic property of gold nanoclusters: Evidence of an electron relay effect *Appl. Phys. A- Mater.* **80** 797
8. Khan M M, Lee J and Cho M H 2014 Au@TiO2 nanocomposites for the catalytic degradation of methyl orange and methylene blue: An electron relay effect *J. Ind. Eng. Chem.* **20** 1584
9. Khan M M, Kalathil S, Han T H, Lee J and Cho M H 2013 Positively charged gold nanoparticles synthesized by electrochemically active biofilms-a biogenic approach *J. Nanosci. Nanotechnol.* **13** 6079
10. He S, Fei Z, Li L, Sun B, Feng X and Ji W 2013 Synthesis and catalytic activity of $M@SiO_2$ (M = Ag, Au, and Pt) nanostructures via "core to shell" and "shell then core" approaches *Chin. J. Catal.* **34** 2098
11. Edison T J I and Sethuraman M G 2012 Instant green synthesis of silver nanoparticles using Terminalia chebula fruit extract and evaluation of their catalytic activity on reduction of methylene blue *Process Biochem.* **47** 1351
12. Singha H P, Gupta N, Sharma S K and Sharma R K 2013 Synthesis of bimetallic Pt–Cu nanoparticles and their application in the reduction of rhodamine B *Colloids Surf., A* **416** 43
13. Amir M, Kurtan U and Baykal A 2015 Synthesis and application of magnetically recyclable nanocatalyst Fe_3O_4@Nico@Cu in the reduction of azo dyes *Chin. J. Catal.* **36** 1280
14. Bastus N G, Merkocį F, Piella J and Puntes V 2014 Synthesis of Highly Monodisperse Citrate-Stabilized Silver Nanoparticles of up to 200 nm: Kinetic Control and Catalytic Properties *Chem. Mater.* **26** 2836

15. Zhang Z Y, Shao C L, Zou P, Zhang P and Zhang M Y 2011 *In situ* assembly of well-dispersed gold nanoparticles on electrospun silica nanotubes for catalytic reduction of 4-nitrophenol *Chem. Commun.* **47** 3906
16. Jiang Z-J, Liu C-Y and Sun L-W 2005 Catalytic Properties of Silver Nanoparticles Supported on Silica Spheres *J. Phys Chem. B* **109** 1730
17. Daniel M C and Astruc D 2004 Gold nanoparticles: Assembly, supramolecular chemistry, quantum-size-related properties, and applications toward biology, catalysis, and nanotechnology *Chem. Rev.* **104** 293
18. Azad U P, Ganesan V and Pal M 2011 Catalytic reduction of organic dyes at gold nanoparticles impregnated silica materials: Influence of functional groups and surfactants *J. Nanopart. Res.* **13** 3951
19. Miah A T, Malakar B and Saikia P 2015 Superior Activity of $Au/CeO_2/SiO_2$ Catalyst for CO Oxidation Reaction *B Catal. Soc. Ind.* **13** 1
20. Saikia P, Miah A T, Malakar B and Bordoloi A 2015 Enhanced Catalytic Activity of Supported Gold Catalysts for Oxidation of Noxious Environmental Pollutant CO *Ind. J. Mater. Sci.* **2015** 1
21. Liu X Y, Wang A, Zhang T and Mou C-Y 2013 Catalysis by gold: New insights into the support effect *Nano Today* **8** 403
22. Ta N, Liu J, Chenna S, Crozier P A, Li Y, Chen A and Shen W 2012 Stabilized Gold Nanoparticles on Ceria Nanorods by Strong Interfacial Anchoring *J. Am. Chem. Soc.* **134** 20585
23. Guo Y Q, Xu K, Wu C Z, Zhao J Y and Xie Y 2015 Surface chemical-modification for engineering the intrinsic physical properties of inorganic two-dimensional nanomaterials *Chem. Soc. Rev.* **44** 637
24. Wang Q, Li Y, Liu B, Dong Q, Xu G, Zhang L and Zhang J 2015 Guangran Xu, Li Zhang and Jun Zhang, Novel recyclable dual-heterostructured Fe_3O_4@CeO_2/M (M = Pt, Pd and Pt–Pd) catalysts: Synergetic and redox effects for superior catalytic performance *J. Mater. Chem. A* **3** 139
25. Lim K, Kim T, Paik S, Haam S, Huh Y M and Lee K 2015 Nanomaterials for Theranostics: Recent Advances and Future Challenges *Chem. Rev.* **115** 327
26. Li G, Zhang D and Yu J C 2009 Thermally stable ordered mesoporous CeO_2/TiO_2 visible-light photocatalysts *Phys. Chem. Chem. Phys.* **11** 3775
27. Wang Y, Li B, Zhang C, Cui L, Kang S, Li X and Zhou L 2013 Ordered mesoporous CeO_2-TiO_2 composites: Highly efficient photocatalysts for the reduction of CO_2 with H_2O under simulated solar irradiation *Appl. Catal. B- Environ.* **130–131** 277
28. Martinez-Arias A, Fernandez-Garcia M, Salamanca L N, Valenzuela R X, Conesa J C and Soria J J 2000 Structural and Redox Properties of Ceria in Alumina-Supported Ceria Catalyst Supports *J. Phys. Chem. B* **104** 4038
29. Sinha A K and Suzuki K 2005 Preparation and Characterization of Novel Mesoporous Ceria-Titania *J. Phys. Chem. B* **109** 1708
30. Liu H, Wang M, Wang Y, Liang Y, Cao W and Su Y 2011 Ionic liquid-templated synthesis of mesoporous CeO_2–TiO_2 nanoparticles and their enhanced photocatalytic activities under UV or visible light *J. Photochem. Photobiol. A* **223** 157
31. Zhu H Q, Qin Z F, Shan W J, Shen W J and Wang J G 2004 Pd/CeO_2–TiO_2 catalyst for CO oxidation at low temperature: A TPR study with H_2 and CO as reducing agents *J. Catal.* **225** 267
32. Miah A T, Malakar B and Saikia P 2016 Gold over Ceria-Titania Mixed Oxides: Solar Light Induced Catalytic Activity for Nitrophenol Reduction *Catal. Lett.* **146** 291
33. Sudarsanam P, Mallesham B, Reddy P S, Großmann D, Grünert W and Reddy B M 2014 Nano-Au/CeO2 catalysts for CO oxidation: Influence of dopants (Fe, La and Zr) on the physicochemical properties and catalytic activity *Appl. Catal. B- Environ.* **144** 900
34. Zhang Y, Zhao G, Zhang Y and Huang X 2014 Highly efficient visible-light-driven photoelectrocatalytic selective aerobic oxidation of biomass alcohols to aldehydes *Green Chem.* **16** 3860
35. Fernandez-Gonzalez R, Julian-Lopez B, Cordoncillo E and Escribano P 2011 New insights on the structural and optical properties of Ce–Ti mixed oxide nanoparticlesdoped with praseodymium *J. Mater. Chem.* **21** 497
36. Fu Q, Kudriavtseva S, Saltsburg H and Flytzani-Stephanopoulos M 2003 Gold-ceria catalysts for low-temperature water-gas shift reaction *Chem. Eng. J.* **93** 41
37. Wang M M, He L, Liu Y M, Cao Y, He H Y and Fan K N 2011 Gold supported on mesostructured ceria as an efficient catalyst for the chemoselective hydrogenation of carbonyl compounds in neat water *Green Chem.* **13** 602
38. Reddy B M, Saikia P, Bharali P, Yamada Y, Kobayashi T, Muhler M and Grunert W 2008 Structural Characterization and Catalytic Activity of Nanosized Ceria-Terbia Solid Solutions *J. Phys. Chem. C* **112** 16393
39. Rastogi P K, Yadav D K, Pandey S, Ganesan V, Sonkar P K and Gupta R 2016 Synthesis and characterization of gold nanoparticles incorporated bentonite clay for electrocatalytic sensing of arsenic(III) *J. Chem. Sci.* **128** 349
40. Han M, Wang X, Shen Y, Tang C, Li G and Smith R L 2010 Preparation of Highly Active, Low Au-Loaded, Au/CeO_2 Nanoparticle Catalysts That Promote CO Oxidation at Ambient Temperatures *J. Phys. Chem. C* **114** 793
41. Wu Y, Liu H, Zhang J and Chen F 2009 Enhanced Photocatalytic Activity of Nitrogen doped Titania by Deposited with Gold *J. Phys. Chem. C* **113** 14689
42. Ke X, Zhang X, Zhao J, Sarina S, Barry J and Zhu H 2013 Selective reductions using visible light photocatalysts of supported gold nanoparticles *Green Chem.* **15** 236
43. Jana N R, Sau T K and Pal T 1999 Growing Small Silver Particle as Redox Catalyst *J. Phys. Chem. B* **103** 115
44. Ahmed K B A, Subramanian S, Sivasubramanian A, Veerappan G and Veerappan A 2014 Preparation of gold nanoparticles using Salicornia brachiata plant extract and evaluation of catalytic and antibacterial activity *Spectrochim. Acta A* **130** 54
45. Gan Z, Zhao A, Zhang M, Tao W, Guo H, Gao Q, Mao R and Liu E 2013 Controlled synthesis of Au-loaded Fe3O4@C composite microspheres with superior SERS

detection and catalytic degradation abilities for organic dyes *Dalton Trans.* **42** 8597
46. Sreekanth T V M, Jung M-J and Eom I-Y 2016 Green synthesis of silver nanoparticles, decorated on graphene oxide nanosheets and their catalytic activity *Appl. Surf. Sci.* **361** 102
47. Zheng Y and Wang A 2012 Ag nanoparticle-entrapped hydrogel as promising material for catalytic reduction of organic dyes *J. Mater. Chem.* **22** 16552
48. Ji Z, Shen X, Xu Y, Zhu G and Chen K 2014 Anchoring noble metal nanoparticles on CeO_2 modified reduced graphene oxide nanosheets and their enhanced catalytic properties *J. Colloid Interf. Sci.* **432** 57
49. Charanpahari A, Ghugal S G, Umare S S and Sasikala R 2015 Mineralization of malachite green dye over visible light responsive bismuth doped TiO_2-ZrO_2 ferromagnetic nanocomposites *New J. Chem.* **39** 3629
50. Li S, Li H, Liu J, Zhang H, Yang Y, Yang Z, Wanga L and Wang B 2015 Highly efficient degradation of organic dyes by palladium nanoparticles decorated on 2D magnetic reduced graphene oxide nanosheets *Dalton Trans.* **44** 9193
51. Kundu S, Mukadam M D, Yusuf S M and Jayachandran M 2013 Formation of shape-selective magnetic cobalt oxide nanowires: Environmental application in catalysis studies *CrystEngComm* **15** 482
52. Ganapuram B R, Alle M, Dadigala R, Dasari A, Maragoni V and Guttena V 2015 Catalytic reduction of methylene blue and Congo red dyes using green synthesized gold nanoparticles capped by salmalia malabarica gum *Int. Nano Lett.* **5** 215
53. Siddhardha R S S, Kumar V L, Kaniyoor A, Muthukumar V S, Ramaprabhu S, Podila R, Rao A M and Ramamurthy S S 2014 Synthesis and characterization of gold graphene composite with dyes as model substrates for decolorization: A surfactant free laser ablation approach *Spectrochim. Acta A* **133** 365
54. Li J, Liu C-Y and Liu Y 2012 Au/graphene hydrogel: synthesis, characterization and its use for catalytic reduction of 4-nitrophenol *J. Mater. Chem.* **22** 8426
55. Mignani A, Fazzini S, Ballarin B, Boanini E, Cassani M C, Maccato C, Barreca D and Nanni D 2015 Mild fabrication of silica-silver nanocomposites asactive platforms for environmental remediation *RSC Adv* **5** 9600
56. Yao T, Cui T, Wang H, Xu L, Cui F and Wu J 2014 A simple way to prepare Au@polypyrrole/Fe3O4 hollow capsules with high stability and their application in catalytic reduction of methylene blue dye *Nanoscale* **6** 7666
57. Panacek A, Prucek R, Hrbac J, Nevecna T, Steffkova J, Zboril R and Kvítek L 2014 Polyacrylate-Assisted Size Control of Silver Nanoparticles and Their Catalytic Activity *Chem. Mater* **26** 1332
58. Narayanan R K, Devaki S J and Rao T P 2014 Robust fibrillar nanocatalysts based on silver nanoparticle-entrapped polymeric hydrogels *Appl. Catal. A- Gen.* **483** 31
59. Khataee A R and Kasiri M B 2010 Photocatalytic degradation of organic dyes in the presence of nanostructured titanium dioxide: Influence of the chemical structure of dyes *J. Mol. Catal. A- Chem.* **328** 8
60. Chen M, Liu P, Wang C, Renab W and Diao G W 2014 Fast catalytic reduction of an azo dye by recoverable and reusable Fe3O4@PANI@Au magnetic composites *New J. Chem.* **38** 4566
61. Megarajan S, Ahmed K B A, Reddy G R K, Kumar P S and Anbazhagan V 2016 Phytoproteins in green leaves as building blocks for photosynthesis of gold nanoparticles: An efficient electrocatalyst towards the oxidation of ascorbic acid and the reduction of hydrogen peroxide *J. Photochem. Photobiol. B* **155** 7
62. Vinodkumar T, Naga Durgasri D, Maloth S and Reddy B M 2015 Tuning the structural and catalytic properties of ceria by doping with Zr^{4+}, La^{3+} and Eu^{3+} cations *J. Chem. Sci.* **127** 1145